



The Resistance of TiN Coatings to Solid Particle Erosion Using Different Deposition Methods

Chunyu Feng · Qi Xie · Lei Yang · Cong Shen · Xin Wei

Submitted: 13 March 2020 / Published online: 7 August 2020
© ASM International 2020

Abstract It was found that the corrosion resistance of WC was significantly improved with the addition of a TiN coating. Erosion testing was done using solid particles to quantify dynamic erosion processes in TiN-coated specimens. TiN coatings were deposited on different specimens using physical vapor deposition (PVD), chemical vapor deposition (CVD), or plasma chemical vapor deposition (PCVD). Results from the erosion tests indicated that the corrosion resistances of the WC-Co cemented carbide samples were improved following all three coating processes. The order of corrosion resistance in terms of strength was TiN-PVD > TiN-CVD > TiN-PCVD > uncoated specimen. The TiN-PVD sample also had the highest resistance to erosion of the three sample types. The principal factors that influence erosion resistance are adhesion forces and the ratio of the hardness (H) of a material to the elastic modulus (E) of the material. Experimental results from this study demonstrated that the TiN-PVD sample had a large adhesion force (42 N) and higher H/E and H^3/E^2 values relative to the other sample types.

Keywords TiN coating · Erosion resistance · Mechanical properties

Introduction

A specialized, cage-type throttle valve is frequently used during natural gas exploitation to balance the pressure difference between the high pressure gas at the bottom of a well and the allowable pressure value in a pipeline before the pipeline reaches a treatment plant. High pressure gases can adversely impact the throttle valve spool, and failures due to the erosion of an alloy are becoming increasingly common. Results from the current study suggest that the loss of the surface of the natural gas spool material found in the spool during throttling is due to fatigue cracking and erosion and oxidation reactions. Surface coatings could be used to improve the erosion resistance of cemented carbide valve core surfaces and could aid in the inhibition of oxidative phenomena. A matrix matching study, based on the physical and mechanical properties of candidate coating materials, was done to identify TiN coating materials that could be appropriate for real-world use.

TiN coatings are widely used for the protection of tools [1–3]. These coatings generally have high hardness values, low coefficients of friction, and good corrosive and oxidative wear resistances [4–7]. TiN coatings can improve the erosion resistance of a material significantly [8, 9]. TiN coatings applied using different coating processes can have different mechanical and material properties, such as mean crystallite sizes, hardness, Young's modulus values, or adhesion properties. The current study characterizes the corrosion and erosion resistances of three TiN coatings that were deposited using PVD, CVD or PCVD.

C. Feng
Key Laboratory of Oil and Natural Gas Equipment, Ministry of Education, Chengdu 610500, People's Republic of China

C. Feng · Q. Xie (✉) · X. Wei
School Mechatronic Engineering, Southwest Petroleum University, Chengdu 610500, People's Republic of China
e-mail: 779437615@qq.com

L. Yang · C. Shen
PetroChina Tarim Oilfield Company, Korla 841000, People's Republic of China

Experiments

Materials

WC-Co cemented carbides were used as substrate materials. The chemical compositions of the WC-Co cemented carbides are presented in Table 1. All specimens (30.0 mm × 30.0 mm × 5.00 mm) were polished by a series of emery papers that were 120, 320 and 600 grit. A final step was performed with diamond grinding paste to achieve a roughness of $R_a \leq 0.08 \mu\text{m}$. Prior to coating, all substrates were thoroughly degreased, ultrasonically cleaned, rinsed with alcohol, and dried by warm air (WC hardness measurements are shown in Table 2).

Deposition and Characterization of the TiN Coatings

PVD coating has three methods: vacuum evaporation, ion plating and sputter coating. The coating density, deposition rate and coating uniformity obtained using ion plating are significantly higher than can be obtained using the other two methods. Therefore, we chose ion plating for PVD in this study.

The TiN coatings for the different specimens were deposited by PVD, CVD, or PCVD. The coated specimens were subsequently coded as TiN-PVD, TiN-CVD or TiN-PCVD, where TiN-PVD means TiN coating that was deposited by physical vapor deposition, TiN-CVD means TiN coating that was deposited by chemical vapor deposition, and TiN-PCVD means TiN coating that was applied using plasma chemical vapor deposition. Uncoated specimens were also tested.

The parameters used to control the PVD, CVD, and PCVD deposition processes are shown in Tables 3, 4 and 5.

The mechanical properties of the TiN coatings that were deposited on the specimens are shown in Table 6. The grain size was determined using the Scherrer equation and reflex parameters (location and FWHM) that were obtained using a Gaussian fit [10]. The sizes of the TiN crystallites obtained using the deposition methods of PVD, CVD, and PCVD were estimated to be approximately 23, 30, and 25 nm, respectively. The coating morphologies and thicknesses were measured using a JEOL JSM 5500LV Scanning Electron Microscope (SEM). Figure 1 shows a representative cross-sectional image of the surface of a TiN coating. Hardness measurements were taken using a

Vivtorinox hardness tester. The Young's modulus values were determined using nanoindentation measurements. The measured hardness and Young's modulus values are shown in Table 6.

Scratch tests were done using a Revetest[®] produced by CSEM to quantify the adhesion of the coating to the substrate [11]. A diamond indenter with a radius of 200 μm was used, and measurements were taken for a normal loading rate of 100 N/min, a scratch speed of 5 mm/min

Table 2 WC hardness measurements

	5 point hardness measurement/HV					Average value/HV
WC	1720	1732	1716	1691	1732	1718.2

Table 3 Process parameters for the TiN coatings prepared using PVD

Coating temperature/ °C	Working vacuum/ Pa	N ₂ flow/ sccm	Cleaning bias duty cycle/V	Coating bias duty cycle/V	Ti target current/ A	Time/ min
200	1–2	400	80%	40%	90	60

Table 4 Process parameters for the TiN coatings prepared using CVD

Deposition temperature/ °C	Deposition pressure/ MPa	Deposition time/min	N ₂ flow/L/ min	H ₂ flow/L/ min	TiCl ₄ flow/L/ min
1000	– 0.05	60	5	5	1.5

Table 5 Process parameters for the TiN coatings prepared using PCVD

Furnace temperature/ °C	Voltage/ V	Current/ A	Deposition time/min	TiCl ₄ flow/ mL/min	H ₂ :N ₂
550	1500	0.3	30	1–2	1:1

Table 6 Properties of the TiN coatings

	PVD	PCVD	CVD
Mean crystallite size (nm)	23 ± 2	30 ± 2	25 ± 2
Coating thickness (μm)	3.6	3.4	3.5
Hardness (HV)	2280	2266	2238
Young's modulus (GPa)	483	591	535
Adhesion (N)	42	37	40

Table 1 The chemical composition of the WC-Co cemented carbides

Quality percentage composition/wt.%	
WC	Co
94	6

and a scratch length of 5 mm. For each TiN-PVD, TiN-PCVD and TiN-CVD sample, at least two scratch tests were performed. The critical loads, LC_2 , at which the removal of the coating from the inside of the scratch began, were 42 N, 37 N and 40 N for the TiN-PVD, TiN-PCVD and TiN-CVD samples, respectively (Fig. 2).

TiN - PVD TiN - PCVD TiN - CVD

Erosion Tests

Solid particle erosion tests were used to quantify the dynamic erosion of the coated specimens. SiC particles (~ 90 μm with a Mohr’s hardness of 9.5) were used as eroding carriers that impinge on each coated specimen at a mass flow rate of approximately 4.5 g/min. The average size of the particles was 120 μm, and the erosion pressure was held at 0.7 MPa using an air compressor. The average particle velocity was 83 m/s, and the distance between the nozzle tip and each specimen was 25 mm. The internal diameter of the nozzle was 2 mm, and the impact angle was fixed at an angle normal to the sample at 90°. The erosion rate was derived based on the depth of the erosion pit in the specimen. The depth of the erosion pit in the specimen was measured using a Veeco NT9300 optical interferometer. All specimens were thoroughly degreased,

ultrasonically cleaned, rinsed with alcohol, and dried by warm air prior to erosion testing. The rate of erosion rate can be calculated using

$$Er = \frac{d}{t}, \tag{Eq 1}$$

where Er is the erosion rate, d is the depth of the erosion pit, and t is the erosion time. Diagram depicting the working principle for gas blasting equipment is shown in Fig. 3.

Results and Discussion

Discussion and Results from the Erosion Tests

The profiles depicting the depths of the erosion pits for the TiN-coated and uncoated specimens, after 100 s of erosion testing, are shown in Fig. 4. The profiles from all of the specimens show a “V-shape” due to the brittleness of the materials [12]. After 100 s of erosion testing, the depth of the erosion pit for the uncoated specimen was the highest (1.98 μm). The depths of the erosion pits for the uncoated, TiN-PVD, TiN-PCVD and TiN-CVD samples were 1.98, 0.9, 1.31 and 1.34 μm, respectively.

Figure 5 shows the depth of erosion as a function of time. During the first 50 s, the surface of the sample is flat, and the material erodes easily. The rate of erosion for the uncoated specimen during the first 50 s was greater than the rate of erosion for the remaining time. During the first 100 s, the rate of erosion for the TiN-PCVD sample was the same as the erosion rate for the TiN-CVD sample. After 100 s, the rate of erosion for the TiN-PCVD sample was higher than the rate of erosion for the TiN-CVD sample. At 250 s, the rate of erosion for the TiN-PCVD sample increased suddenly. The increase in rate is likely due to wear of the coating. A similar, sudden increase in the rate of erosion was observed for the TiN-CVD sample at 275 s.

The average rates of erosion for the TiN-coated and uncoated specimens, based on 300 s erosion tests, are shown in Fig. 6. The rate of erosion for the uncoated specimen was the highest observed rate among all of the experimental specimens. The TiN-PVD specimen had the minimum rate of erosion.

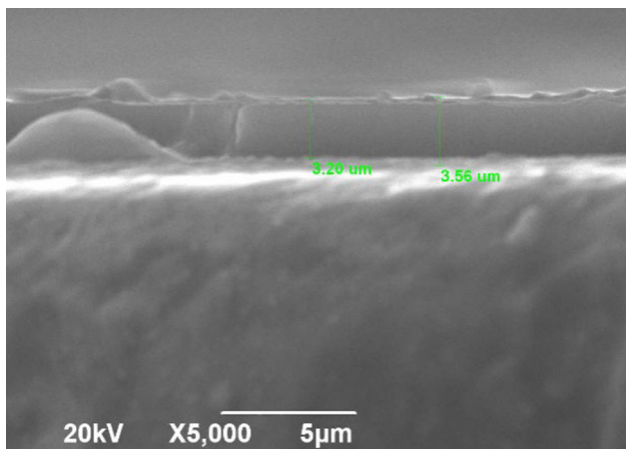


Fig. 1 Cross-sectional image of the surface coating deposited using TiN-PVD

Fig. 2 Damage to the TiN coatings during the scratch tests

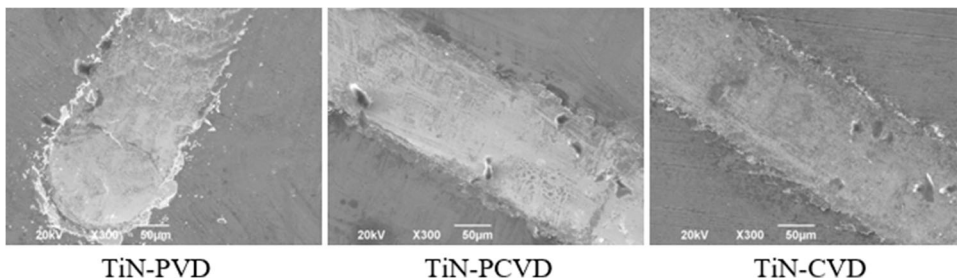


Fig. 3 Diagram depicting the working principle for gas blasting equipment

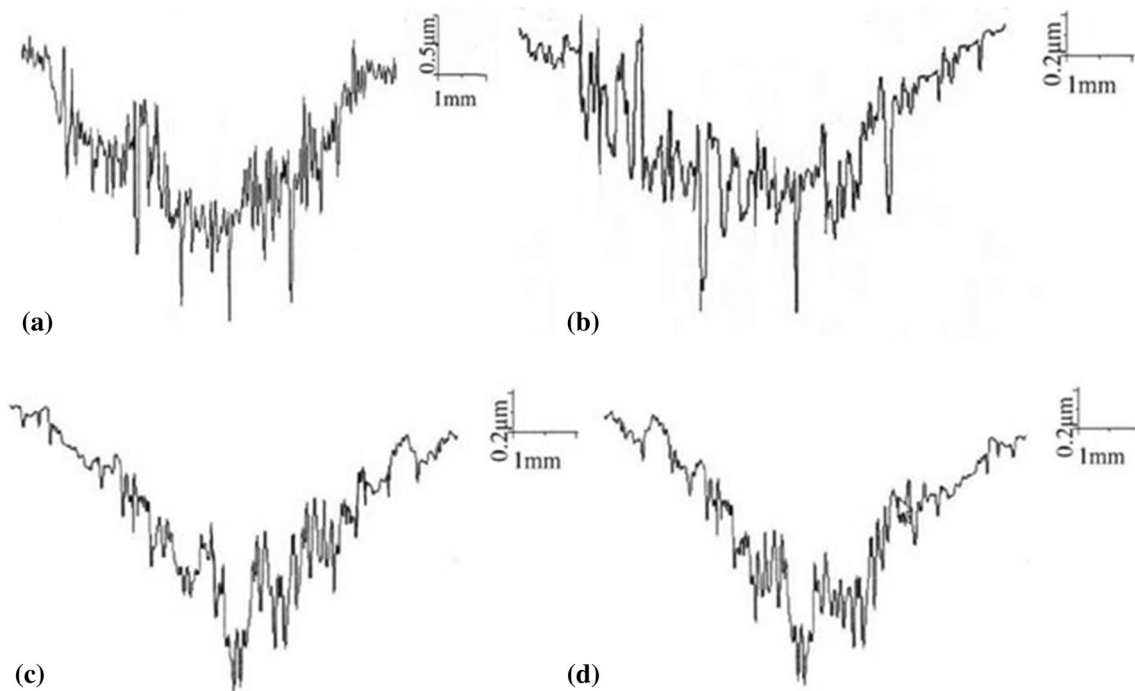
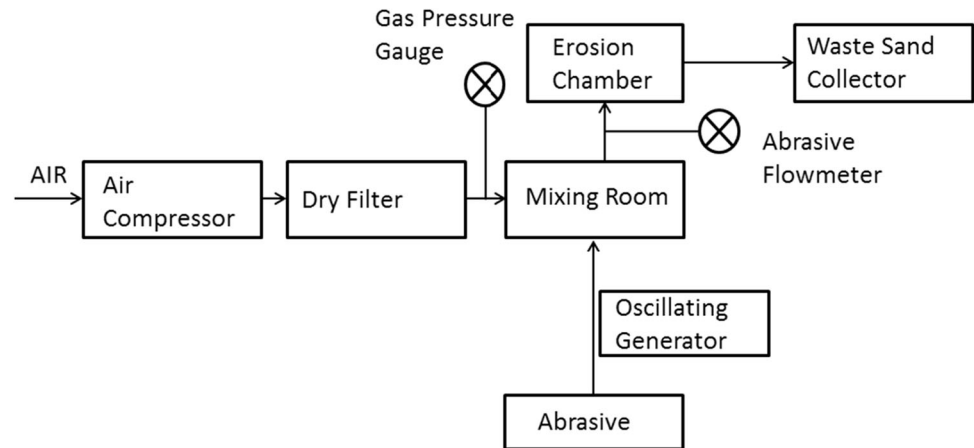


Fig. 4 Erosion pit profiles for an (a) uncoated specimen, (b) a TiN-PVD specimen, (c) a TiN-PCVD specimen, (d) TiN-CVD specimen

Effects of Mechanical Properties on Erosion Resistance

Figure 7 shows the relationships between adhesion and erosion rates for the three specimen types used in this study. In Fig. 7, the TiN-PVD samples had the greatest amount of adhesion (42 N), followed by the TiN-CVD samples (40 N), then the TiN-PCVD samples (37 N). Consequently, the rate of erosion of the coatings can be inferred to largely depend on its adhesive properties. Figure 8 illustrates the observed relationships between hardness and the rates of erosion for the three types of specimens. The rates of erosion for the three coated samples were not fully consistent with the observed increases

in the hardness of the coating. The PCVD coating had hardness values that were higher than the hardness values for the CVD coating, but the rate of erosion for the former was higher than that of the latter. One possible reason for the inconsistency was the mean crystallites size. The mean crystallites size of the PCVD coating was 30 nm, while the mean crystallites size of the CVD coating was 25 nm. For solid particle erosion experiments, larger crystallites can be cut more easily and could lead to a higher rate of erosion.

Previous studies in the literature suggested that the main factors that influence the erosion resistance of coatings are hardness (H), elastic modulus (E), and adhesion parameters. Shtansky [13] suggested using the value of H/E to

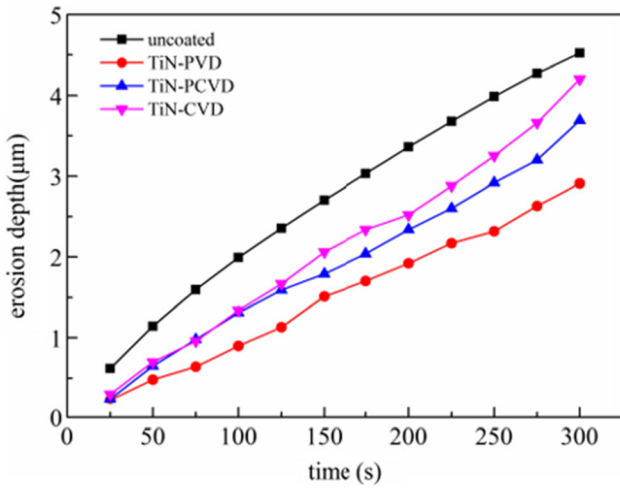


Fig. 5 Curves depicting the depth of erosion for the uncoated specimen and the TiN-coated specimens

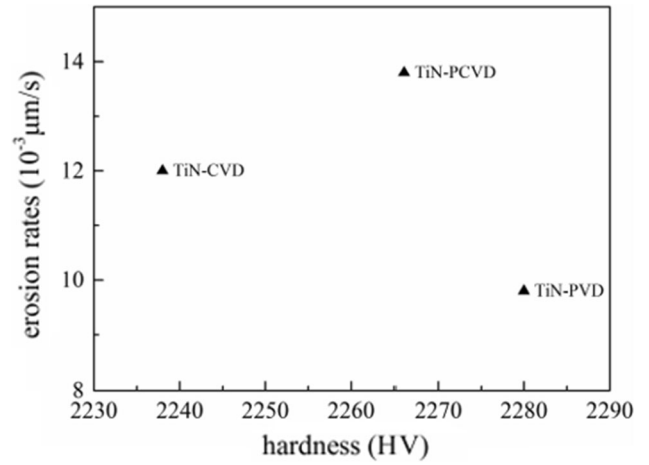


Fig. 8 Erosion rates as a function of hardness for the three TiN coating types

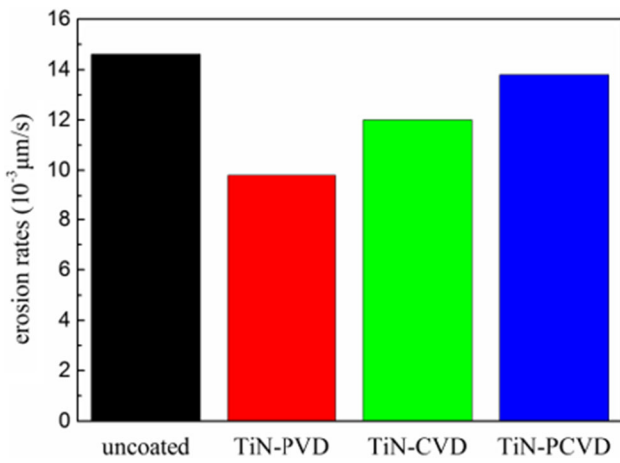


Fig. 6 Rates of erosion rates for the uncoated and three TiN-coated samples

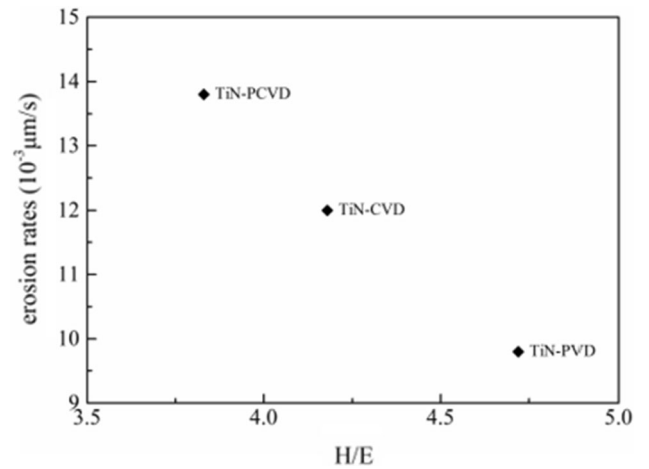


Fig. 9 H/E ratios and erosive wear rates for the three different coating processes

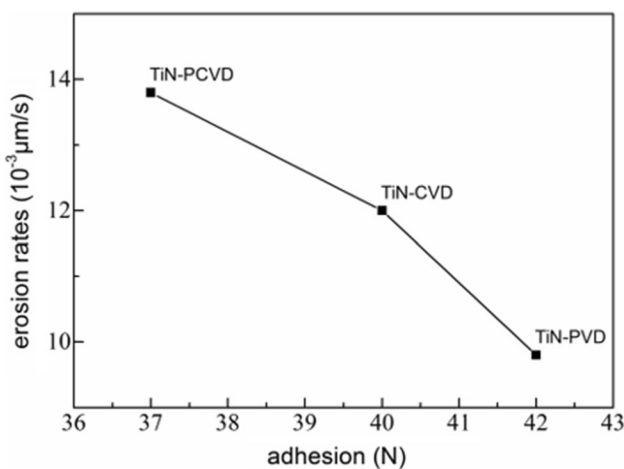


Fig. 7 Erosion rates as a function of adhesion for three TiN coatings on a film substrate

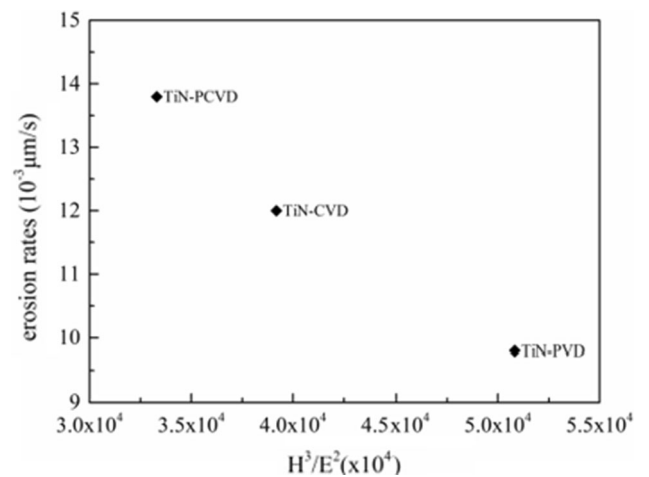


Fig. 10 H^3/E^2 ratios and erosive wear rates for the three different coating processes

represent the capacity for non-elastic strain, while Musil [14] recommended the use of the quantity H^3/E^2 to represent the capacity for resistance to plastic deformation. As the values of H^3/E^2 increase, the resistance to cracking improves. Musil [14] further suggested that higher H/E or higher H^3/E^2 values result in a lower rate of erosion. Figure 8 depicts the relationships between H/E , H^3/E^2 and the rates of erosion for the three coating types used in this study. The TiN-PVD samples had higher H/E and H^3/E^2 values and a lower rate of erosion than the TiN-PCVD and TiN-CVD samples had. The rates of erosion (Er) for the three coating types decreased with increases in the H/E and H^3/E^2 ratios, as shown in Figs. 9 and 10.

The relationship between Er and H/E can be expressed as

$$Er = A(H/E)^{-B}, \quad (\text{Eq 2})$$

where A and B are constants and the values are determined based on the properties of the coating and the substrate.

Conclusions

In this study, TiN coatings were deposited on substrates using PVD, CVD, or PCVD. Results from solid particle erosion tests suggest that the corrosion resistance of WC-Co cemented carbides can be improved by using coatings of TiN-PCVD, TiN-CVD, or TiN-PVD. The TiN-PVD samples had the highest corrosion resistances followed by, in order of decreasing corrosion resistance, the TiN-CVD, TiN-PCVD, and uncoated samples. The TiN-PVD samples also had the highest erosion resistance among the three types of coated specimens. The TiN-PVD samples likely had the highest corrosion and erosion resistances since the TiN-PVD samples had the highest adhesion forces (42 N) and had higher H/E and H^3/E^2 values than the TiN-PCVD and TiN-CVD samples.

Acknowledgments This work was supported by the Open Fund (OGE201702-05) of the Key Laboratory of Oil and Gas Equipment, Ministry of Education (Southwest Petroleum University).

References

1. M.W. Reedy, T.J. Eden, J.K. Potter, D.E. Wolfe, Erosion performance and characterization of nanolayer (Ti, Cr)N hard coatings for gas turbine engine compressor blade applications. *Surf. Coat. Technol.* **206**, 464–472 (2011)
2. E. Bousser, M. Benkahoul, L. Martinu, J.E. Klemberg-Sapieha, Effect of microstructure on the erosion resistance of Cr-Si-N coatings. *Surf. Coat. Technol.* **203**, 776–780 (2008)
3. Y. Gachon, P. Jenny, A. Former, G. Farges, M.C. Sainte Catherine, A.B. Vannes, Erosion by solid particles of W/W–N multilayer coatings obtained by PVD process. *Surf. Coat. Technol.* **113**, 140–148 (1999)
4. K. Alicja, C. Andrzej, Influence of the substrate hardness on the cavitation erosion resistance of TiN coating. *Wear* **263**, 395–401 (2007)
5. L. Fengqun, Yu. Zhiming, The corrosion resistance and wear resistance of thick TiN coatings deposited by arc ion plating. *Surf. Coat. Technol.* **145**, 80–87 (2001)
6. C. Maurer, U. Schulz, Solid particle erosion of thick PVD coatings on CFRP. *Wear* **317**, 246–253 (2014)
7. A.K. Krella, The new parameter to assess cavitation erosion resistance of hard PVD coatings. *Eng. Fail. Anal.* **18**, 855–867 (2011)
8. H. Cheng-Hsun, C. Ming-Li, L. Kuei-Laing, Corrosion resistance of TiN/TiAlN-coated ADI by cathodic arc deposition. *Mater. Sci. Eng., A* **421**, 182–190 (2006)
9. W.D. Münz, L.A. Donohue, P. Hovsepian, Properties of various large-scale fabricated TiAlN- and CrN-based superlattice coatings grown by combined cathodic arc-unbalanced magnetron sputter deposition. *Surf. Coat. Technol.* **125**, 269–277 (2000)
10. K. Alicja, The experimental resistance parameter for TiN coating to cavitation action. *Adv Mater Sci* **10**, 4–18 (2010)
11. L.C. Hernández, L. Ponce, A. Fundora, E. López, E. Pérez, Nanohardness and residual stress in TiN coatings. *Materials* **4**, 929–940 (2011)
12. D.W. Wheeler, R.J.K. Wood, Erosion of hard surface coatings for use in offshore gate valves. *Wear* **258**, 526–536 (2005)
13. D.V. Shtansky, P. Kiryukhantsev-Korneev, I.A. Bashkova, A.N. Sheveiko, E.A. Levashov, Multicomponent nanostructured films for various tribological applications. *Int J Refract Met H* **28**, 32–39 (2010)
14. J. Musil, Hard and superhard nanocomposite coatings. *Surf. Coat. Technol.* **125**, 322–330 (2000)

Publisher's Note Springer Nature remains neutral with regard to jurisdictional claims in published maps and institutional affiliations.